ChemElectroChem

Chemistry Europe
European Chemical Societies Publishing
ChemElectroChem

RESEARCH ARTICLE OPEN ACCESS

Electrochemical Hofmann Rearrangement to Hydrazides

Zeyu Feng[1] | Darryl F. Nater[1] | Tonin Léautier[1] | Matthieu Sintes[1] | Thomas Weyhermüller[2] | Siegfried R. Waldvogel[1,3]

[1]Department of Electrosynthesis, Max-Planck-Institute for Chemical Energy Conversion, Mülheim an der Ruhr, Germany | [2]Department of Inorganic Spectroscopy, Max-Planck-Institute for Chemical Energy Conversion, Mülheim an der Ruhr, Germany | [3]Institute of Biological and Chemical Systems – Functional Molecular Systems (IBCS FMS), Karlsruhe Institute of Technology (KIT), Karlsruhe, Germany

Correspondence: Siegfried R. Waldvogel (siegfried.waldvogel@cec.mpg.de)

Received: 9 December 2025 | **Revised:** 9 January 2026 | **Accepted:** 12 January 2026

Keywords: electrosynthesis | flow chemistry | Hofmann rearrangement | hydrazides

ABSTRACT

We present the first electrochemical Hofmann rearrangement for the sustainable and safe synthesis of *N*,*N*-disubstituted hydrazides from readily available ureas. The process employs a simple undivided-cell set-up with LiCl as a low-cost, environmentally benign supporting electrolyte and operates efficiently at high current density up to 120 mA/cm^2. This strategy accommodates a broad substrate scope with 36 examples and yields up to 84%. Additionally, the method was found to be both applicable and scalable for pharmaceutically relevant compounds.

1 | Introduction

The first natural product containing a nitrogen—nitrogen (N—N) bond was reported back in 1940, isolated from an Australian cycad plant. Since then, several natural products featuring this moiety have been identified [1]. Beyond their presence in nature, compounds with N—N bonds have attracted considerable attention in both pharmaceuticals and agrochemicals, with an increasing number of related active compounds gaining FDA approval in recent years [2]. At the same time, hydrazine-based compounds have also shown great properties in material science, particularly in the development of organic light-emitting diodes (OLEDs) and covalent organic frameworks(COFs) [3, 4]. However, in contrast to analogous C—C and C—N bonds, the formation of N—N bond has still remained as a major challenge in the synthetic community, owing to the inherent nucleophilicity of nitrogen atoms. Despite this, a significant advancement has been made in the last few decades for the methodologies of N—N bond formation, including but not limited to N-nitration, N-amination, rearrangement, and transition metal catalysis [5–7].

On the other hand, *N*,*N*-disubstituted hydrazides—a representative class of N—N bond–containing compounds—have exhibited indispensable bioactivities and significant synthetic value (Scheme 1), rendering them key target molecules in the construction of N—N bonds. *N*,*N*-Disubstituted hydrazides can be conveniently obtained via acetylation of the corresponding hydrazines. A general approach to access *N*,*N*-disubstituted hydrazines involves the reduction of N-nitrosamines (Scheme 2a). However, this method suffers from several drawbacks: the use of hydride reagents or zinc in acetic acid often limits functional group tolerance. In addition, *N*-nitrosamines are well-known potent carcinogens, and their N—NO bonds are susceptible to cleavage under strongly reducing conditions [8–13]. Alternatively, rearrangement reactions have also been employed as a common strategy to access hydrazides and hydrazines. The Curtius rearrangement can provide hydrazine derivatives; however, this approach has seen limited use, likely due to its potential explosiveness and the low selectivity arising from the rapid dimerization of *N*-isocyanate intermediates [14–16]. In contrast, the Lossen rearrangement, as demonstrated by Beauchemin and coworkers, offers a reliable route to complex hydrazine derivatives. Nevertheless, the required precursors involve multistep syntheses, and the use of bulky leaving groups compromises atom economy (Scheme 2b) [17].

Traditionally, the Hofmann rearrangement has been applied primarily to the synthesis of amines from amides. In general, it can

Zeyu Feng and Darryl F. Nater contributed equally to this study.

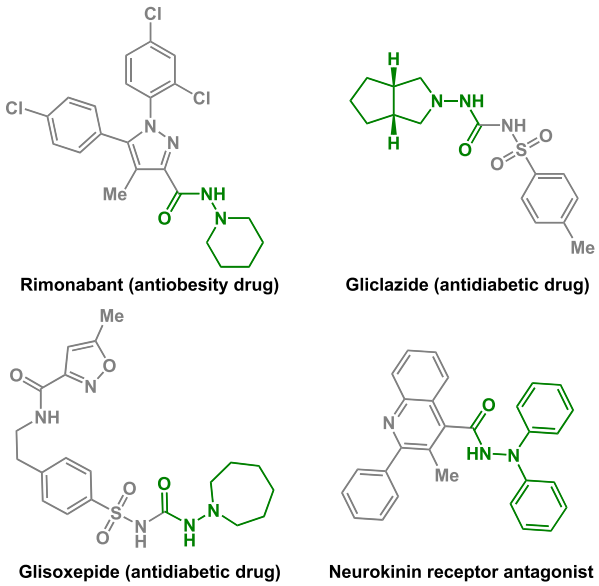

SCHEME 1 | Selected examples of bioactive molecules with a hydrazide structural motif.

also be used directly with readily available ureas as substrates, eliminating the need for prefunctionalization and thereby improving atom economy. To our surprise, reports on employing the Hofmann rearrangement for N—N bond formation are extremely limited. In the few documented examples, environmentally hazardous oxidants were required, and the scope remained narrow —factors that collectively restrict the broader applicability of this approach (Scheme 2b) [18, 19]. In recent years, electrochemical methods have emerged as more sustainable and cost-effective alternatives in organic synthesis [20–26]. A variety of Hofmann-type rearrangements have been successfully adapted to electrochemical conditions [27–33]. Additionally, electrosynthesis has shown great promise in enabling dehydrogenative N—N coupling reactions [34–41]. Previously, no electrochemical protocol has been reported for the Hofmann rearrangement toward the synthesis of hydrazides. To address this gap, we herein present a practical, sustainable, and scalable method for the transformation of readily available 1,1-disubstituted ureas into their hydrazides under mild electrochemical conditions (Scheme 2c). Lithium chloride was used not only as the supporting electrolyte but also as a chlorine source capable of oxidizing the urea substrate [42]. The resulting *N*-chlorourea undergoes in the presence of methoxide a Hofmann-type rearrangement to generate the desired hydrazides. Our method demonstrates remarkable generality by accommodating *N*,*N*-diaryl, *N*,*N*-dialkyl, and *N*-aryl-*N*-alkyl hydrazides, a scope of products unmatched by any previously reported approach.

2 | Results and Discussion

In our previous work, a flow-based electrochemical protocol opting for high current density was developed for the Hofmann rearrangement of carboxamides [27, 28]. Building upon this foundation, we initiated our study using the same setup and analogous reaction parameters (see supporting information). Initial reaction optimization was performed using a *N*,*N*-diarylurea, which was selected as a representative substrate. To mitigate polymerization at the position para of the phenyl ring during electrolysis [43], we employed **1a** *N*,*N*-bis(4-chlorophenyl)urea

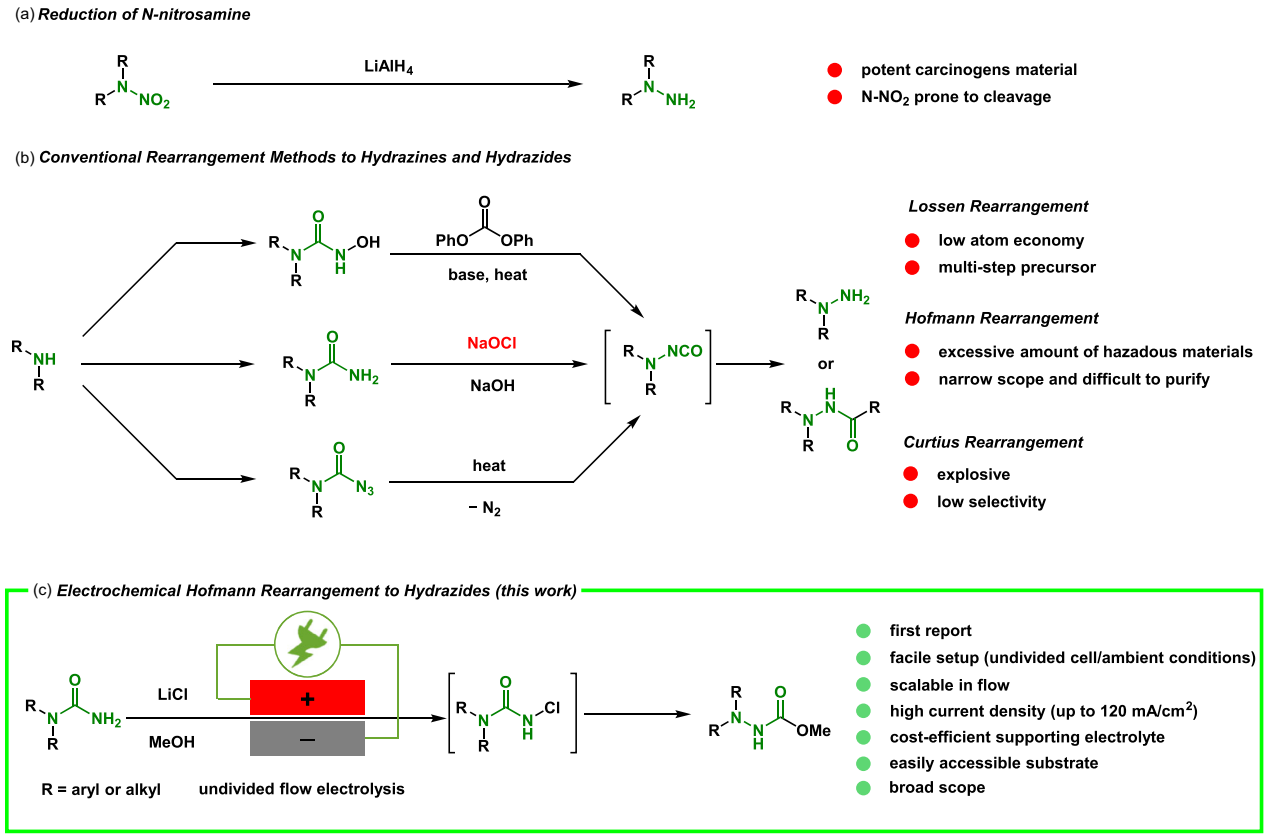

SCHEME 2 | Conventional methods versus electrochemical Hofmann rearrangement for *N*,*N*-disubstituted hydrazides (hydrazines).

instead of the nonfunctionalized *N*,*N*-diphenylurea. Furthermore, Et_4NCl was selected as the supporting electrolyte for the initial screening.

To optimize the reaction parameters, a design of experiments (DoE) study was conducted focusing on four factors: concentration of supporting electrolyte, interelectrode gap, current density, and amount of applied charge [44]. The DoE results revealed that, within the range of 0.05–0.15 M, the supporting electrolyte concentration was the most significant factor positively influencing the yield (see Supporting Information for details). Increased amount of applied charge, larger interelectrode gap, and higher current density also contributed to improved yields, although their effects were less pronounced. Guided by the trends of DoE, further linear optimization was performed, ultimately delivering a very good yield of 87% of **2a** (Figure 1). Meanwhile, single crystals of **2a** suitable for X-ray analysis were obtained by slow evaporation from ethyl acetate. The structure of **2a** was thus unambiguously confirmed by the crystal structure. The length of the newly formed N—N bond was determined to be 1.389 Å, which falls between that of a typical N—N single bond (1.425 Å) and N═N double bond (1.240 Å) [45]. This intermediate bond length is ascribed to the electron-withdrawing effect by the adjacent acyl group, which lowers lone pair repulsion between both nitrogen atoms [46]. In addition, the N—C(O) bond length was measured to be 1.359 Å, comparable to the N1–C5 bond length in pyrazole [45], suggesting partial double bond character due to resonance. This geometric constraint likely restricts free rotation around the N—N bond, which is reflected in the ^1H NMR spectra of **2a**, wherein the methoxy (OCH_3) signal exhibits splitting at room temperature. A similar phenomenon was also observed in our previous study on hydrazides [34].

Replacing the chlorine source, which also serves in a dual role as supporting electrolyte, from Et_4NCl to the more economical and environmentally benign LiCl led to a slight improvement in yield (Entry 2). Increasing the concentration of LiCl to 0.3 M resulted in a more pronounced enhancement of yield to 95% (Entry 6). Interestingly, other halides such as Br^- and I^- (Entry 3), which are often employed in electrochemical Hofmann rearrangements [27–33], gave no conversion in this reaction—likely due to lower oxidative power of bromine and iodine compared to chlorine. Furthermore, we observed that addition of base is crucial for improving the yield (Entry 4), even though methoxide is also generated at the cathode during electrolysis by reduction of the solvent. Notably, the reaction could also be performed under single-pass flow conditions, albeit with a slightly lower yield (Entry 5). Then, we evaluated an ex-cell version of the electrolysis (Entry 7) [47, 48], which afforded only a low yield with significant amounts of nonconverted starting material. This poor performance is likely due to the use of an undivided cell, which allows for electron shuttling between the anode and cathode. Another critical factor that should not be overlooked is poststirring after electrolysis (Entry 8), as the conversion of the intermediate *N*-chloro-urea is typically not fast and requires approximately 2 h at room temperature in the case of the test reaction. No further reaction occurred after stirring the mixture in the absence of electricity for 2 h (Entry 9), which is indicative of the necessity of electrolysis for this transformation.

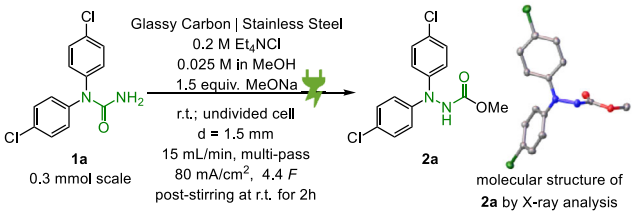

Entry	Deviation	Yield[a]
1	None	87%
2	LiCl instead of Et_4NCl	91%
3	Et_4NBr or Et_4NI instead of Et_4NCl	0%
4	Wihtout MeONa	70%
5	Single pass instead of recirculation	80%
6	**0.3 M LiCl instead of 0.2 M Et_4NCl**	**95%**
7	Ex-cell electrolysis	34%
8	No post-stirring	32%
9	No electricity and stir for 2 h	0%

[a]Yields were determined by GC-FID using pentamethylbenzene as reference

FIGURE 1 | Optimization of reaction conditions.

With the optimal conditions in hand (Figure 1, Entry 6), we proceeded to explore the generality of our methodology. The scope was categorized into three groups: *N*,*N*-diaryl hydrazides, *N*,*N*-dialkyl hydrazides, and *N*-aryl-*N*-alkyl hydrazides (Scheme 3). First, we studied the synthesis of *N*,*N*-diaryl hydrazides, as our test substrate belongs to this category. Common halo substituents such as chloro and bromo were well tolerated at positions para, ortho, and meta on arene moieties, highlighting the potential for further functionalization via cross-coupling reactions. In addition, fluoro-, *tert*-butyl-, and cyano-substituted products were obtained in acceptable to synthetically useful yields, whereas iodo- and nitro-substituted products were isolated in unsatisfactory yields. However, slight modifications were required for substrates (for making e.g., **2g**, **2h**, and **2j**, Scheme 3) involving strong electron-withdrawing groups (EWGs), as within the *N*-chloro-urea intermediate the lone pair on the amine nitrogen is delocalized toward the EWG. Thereby, lowering its nucleophilicity and impeding intramolecular attack at the other nitrogen to facilitate the rearrangement. To overcome this issue, the temperature was raised to 60°C to ensure complete conversion of the intermediate. Nevertheless, the carbazole derivative (**2p**) gave only 32% yield despite the incorporation of two electron-releasing groups and poststirring at 100°C. This unsatisfactory result can be attributed to the extensive conjugation between the lone pair electron on the pyrrolic nitrogen and the π-system. Subsequently, we applied our method to the synthesis of *N*,*N*-dialkyl hydrazides. For this type of substrates, 2.5 *F* as amount of applied charge already proved to be sufficient to deliver satisfactory yields. In recent years, cyclic amines have attracted increasing attention in drug design as privileged building blocks for active pharmaceutical ingredients (APIs) [49–51]. Accordingly, we were interested to see whether our method could also be applied to these substrates. Notably, the hydrazine or hydrazide motifs of certain products presented here (e.g., **3f**, **3j**, and **3k**) have already been incorporated into bioactive molecules [52–55]. In the end, we also evaluated our methods on *N*-aryl-*N*-alkyl ureas. For this class of starting materials, we found that lowering the interelectrode gap from 1.5 to 1.0 mm and increasing the current density to 120 mA cm^{-2} significantly improved the yields. Primary (**4a**) and secondary (**4b**) alkyl substituents were well tolerated under these conditions, whereas tertiary alkyl groups—adamantyl in this case (**4h**)—appeared to define the limitation.

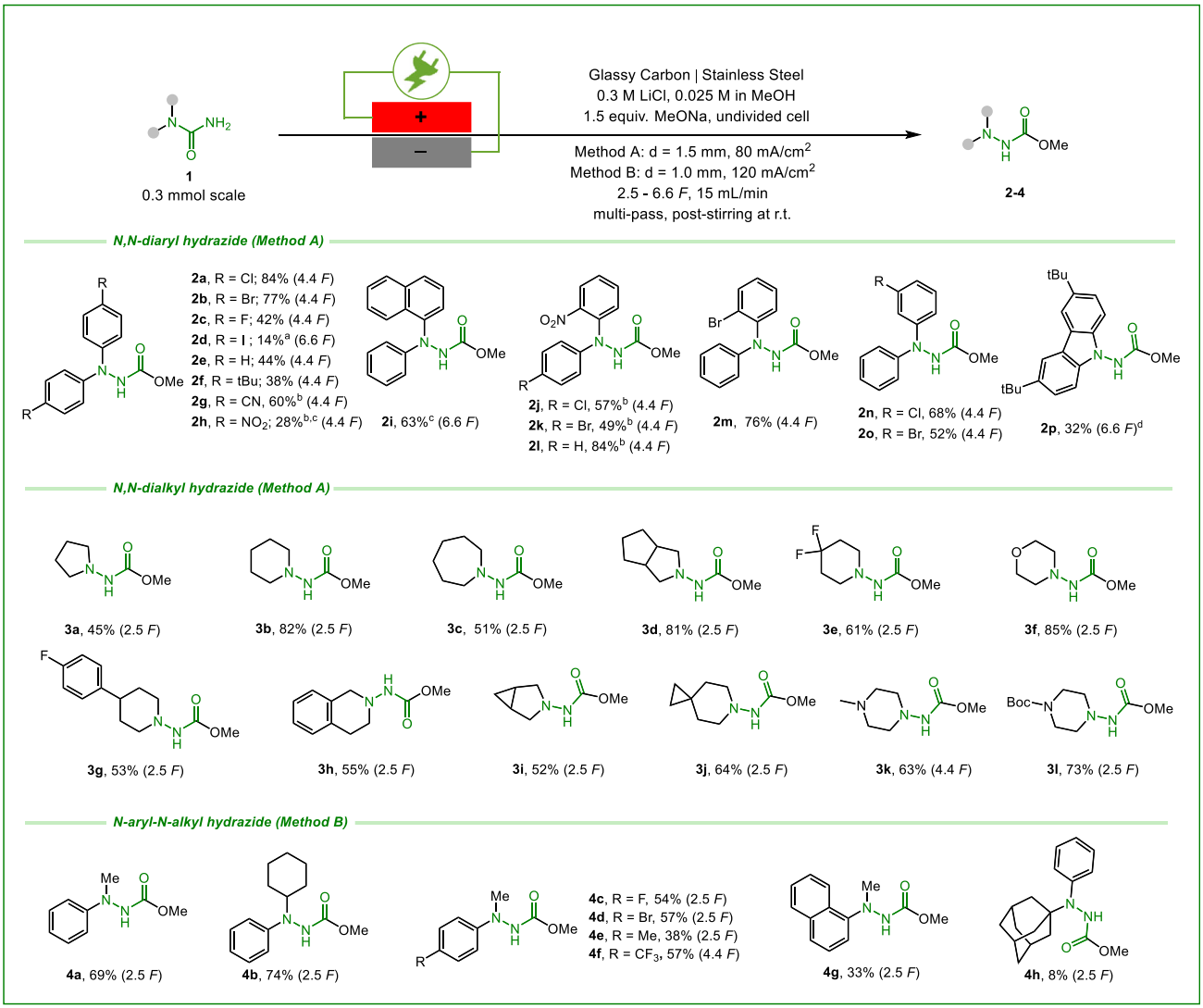

Isolated yields are reported; amount of applied charge in parentheses; [a] MeCN/MeOH (3/7) mixture as solvent; [b] post-stirring at 60 °C; [c] no MeONa was added; [d] THF/MeOH (1/3) mixture as solvent and post-stirring at 100 °C.

SCHEME 3 | Scope of Hofmann rearrangement to hydrazides.

During the exploration of the synthetic scope, an intermediate was detected in certain reactions by TLC-MS, which we hypothesized to be an *N*-chloro-urea, analogous to the *N*-haloamide intermediate in the classical Hofmann rearrangement. To validate this assumption, the intermediate (**int**) was isolated from a reaction of **1h** since the strong electron-withdrawing effect of the two NO_2 groups was expected to deactivate the amine nitrogen and thereby suppress nucleophilic N—N coupling to afford **2h**. This stabilization effect allowed us to purify and characterize this intermediate. Single crystal X-ray analysis confirmed the proposed structure (Scheme 4a) [56]. Subsequent treatment of **int** with 4.4 equiv. MeONa in methanol at 60°C furnished the corresponding hydrazide in 55% [57].

Hydrazides prepared using our method can be readily converted to the corresponding hydrazines by simple basic hydrolysis. For example, treatment of hydrazide **3c** with aqueous base provided hydrazine **5** in high yield (Scheme 4b). Compound **5** is a versatile intermediate: it has been employed as a key building block for the antidiabetic agent tolazamide [58] and serves as a convenient precursor for the synthesis of pyrazole derivatives via standard cyclocondensation protocols [59]. These transformations demonstrate the practical synthetic utility of our hydrazide products for downstream elaboration into pharmaceutically relevant scaffolds. In addition, a scale-up study was performed for the synthesis of hydrazide **3d**. Under the standard electrolysis conditions, the process could be scaled up 25-fold, delivering the desired product in only slightly diminished yield (81%→74%) while requiring an additional 0.2 F amount of applied charge (Scheme 4c). Moreover, the product is simply isolated making this transformation cost-efficient [60]. Based on the identification of the *N*-chloro-urea intermediate, a plausible mechanism for the overall transformation is proposed (Scheme 4d). The sequence closely resembles previously reported electrochemical Hofmann rearrangements [27–33]. In this pathway, a reactive *N*-amino-isocyanate intermediate [61] is formed via the base-promoted rearrangement of **int**. Notably, **int** exhibits a significantly longer lifetime than the other species in the system, and its conversion proceeds rather sluggishly at room temperature for many substrates, necessitating stirring after the end of the electrolysis. Accordingly, we postulate that the rearrangement of **int** to the *N*-amino-isocyanate intermediate constitutes the rate-determining step.

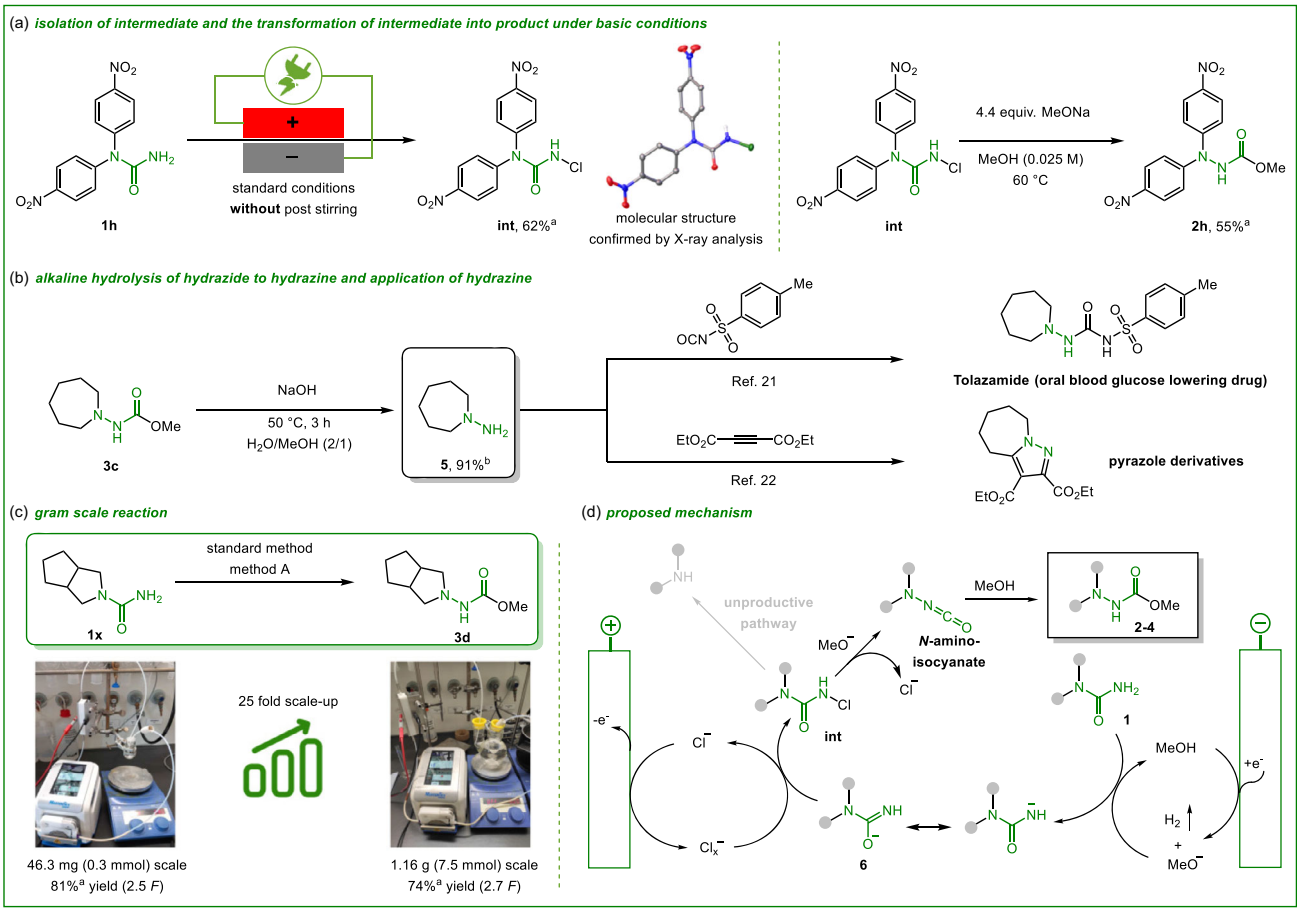

[a]isolated yield; [b]yield determined by ^{1}H NMR with CH_2Br_2 as internal standard

SCHEME 4 | Mechanistic and application investigation.

3 | Conclusion

In summary, we have developed the first electrochemical Hofmann rearrangement for the efficient synthesis of valuable hydrazides, delivering 36 examples with yields of up to 84%. This protocol employs readily accessible *N*,*N*-disubstituted ureas as starting materials and was systematically optimized by DoE. It displays broad generality, tolerating three distinct substrate classes and a wide range of functional groups. A key advantage of this method lies in the dual role of lithium chloride, which simultaneously functions as halogen source and supporting electrolyte, enabling a highly streamlined and economical setup. The reaction is readily scalable, as demonstrated by a 25-fold scale-up with slight increase of the amount of applied charge. The resulting hydrazides show excellent downstream utility, being smoothly converted into hydrazines under basic hydrolysis conditions. Notably, many of the obtained hydrazides are recognized pharmaceutical building blocks, highlighting the strong potential of this strategy for API manufacturing. Moreover, the isolation of the *N*-chloro-urea intermediate offers clear experimental validation of the proposed mechanism. This electrified method can serve to access hydrazine intermediates in a safer and more sustainable manner.

Author Contributions

Z. F., D. F. N., and S. R. W. conceptualized the project. Z. F., T. L., and M. S. conducted the experiments. T. W. conducted the crystallographic analysis. Z. F., D. F. N., and S. R. W. wrote the manuscript, which was revised by all authors. S. R. W. supervised the project. Z. F. and D. F. N. contributed equally. All authors have given approval to the final version of the manuscript.

Acknowledgments

The authors acknowledge financial support by the BMFTR in the frame of the Clusters4future initiative ETOS–Electrifying Technical Organic Synthesis (project HAVANA – FKZ 03ZU1205DD). Support from the MPG for open access is highly appreciated.

Open Access funding enabled and organized by Projekt DEAL.

Funding

This work was supported by the Bundesministerium für Bildung und Forschung (Grant no. HAVANA – FKZ 03ZU1205DD); Max-Planck-Gesellschaft (Grant no. Open Access by DEAL Agreement).

Conflicts of Interest

The authors declare no conflicts of interest.

Data Availability Statement

The data that supports the findings of this study are available in the supplementary material of this article.

References

1. L. M. Blair and J. Sperry, "Natural Products Containing a Nitrogen–nitrogen Bond," *Journal of Natural Products* 76 (2013): 794–812.

2. C. Angeli, S. Atienza–Sanz, S. Schröder, et al., "Access to Nitrogen–nitrogen Bond-Containing Heterocycles through Substrate Promiscuity of Piperazate Synthases," *ACS Catalysis* 15 (2025): 310–342.

3. W.-Y. Liu, Y.-L. Zhang, X. Fei, L.-S. Liao, and J. Fan, "9,9′-Bicarbazole: New Molecular Skeleton for Organic Light-Emitting Diodes, "*Chemistry – A European Journal* 25 (2019): 4501–4508.

4. S. Feng, H. Xu, C. Zhang, et al., "Bicarbazole-Based Redox-Active Covalent Organic Frameworks for Ultrahigh-Performance Energy Storage," *Chemical Communications* 53 (2017): 11334–11337.

5. Q. Guo and Z. Lu, "Recent Advances in Nitrogen–nitrogen Bond Formation," *Synthesis* 49 (2017): 3835–3847.

6. J.-L. Hu, Y. Wu, Y. Gao, Y. Wang, and P. Wang, "Recent Advances in Catalytic Nitrogen–nitrogen Bond Formation Reactions," *ACS Catalysis* 14 (2024): 5735–5778.

7. A. Tabey, P. Y. Vemuri, and F. W. Patureau, "Cross-Dehydrogenative N–N Couplings," *Chemical Science* 12 (2021): 14343–14352.

8. W. O. Kermack, W. H. Perkin, and R. Robinson, "CCXXVI.—Harmine and Harmaline. Part VI. The Synthesis of *N*-Methyltetrahydronorharmine and the Constitution of Harmaline and of the Alkylated Harmines," *Journal of the Chemical Society, Dalton Transactions* 121 (1922): 1872–1896.

9. J. N. Ashley and S. S. Berg, "The Search for Chemotherapeutic Amidines. Part XIV. Congeners of 4: 4′-Diamidinoazobenzene," *Journal of the Chemical Society* (1957): 3089–3093.

10. B. T. Hayes and T. S. Stevens, "Reduction of Nitrosamines to Hydrazines," *Journal of the Chemical Society [Section] C* 8 (1970): 1088–1089.

11. C. Hanna and F. W. Schüler, "The Reaction of Disubstituted Nitrosamines with Lithium Aluminum Hydride," *Journal of the American Chemical Society* 74 (1952): 3693–3694.

12. M. D. Rosa and P. Haberfield, "Nitrous Acid Deamination of 1,1-Disubstituted Aromatic Hydrazines," *Journal of Organic Chemistry* 46 (1981): 2639–2643.

13. R. E. Johnson, A. E. Soria, J. R. O. ´Connor, and R. A. Dobson, "Synthesis and Antibacterial Activity of 1-(arylamino)-1H-Pyrroles and 4-(1H-Pyrrol-1-Ylimino)-2,5-Cyclohexadienes," *Journal of Medicinal Chemistry* 24 (1981): 1314–1319.

14. N. Koga and J.-P. Anselme, "Preparation of 1, 1-Diarylhydrazines," *Journal of Organic Chemistry* 33 (1968): 3963–3964.

15. C. Wentrup, J. J. Finnerty, and R, Koch, Amino-, Alkoxy-, and Alkylthio-Isocyanates and -Isothiocyanates, RX-NCY, Their Isomers RX-YCN and RX-CNY, and Their Rearrangements," *Current Organic Chemistry* 15 (2011): 1745–1759.

16. J.-F. Vincent-Rocan and A. M. Beauchemin, "*N*-Isocyanates, N-Isothiocyanates and Their Masked/Blocked Derivatives: Synthesis and Reactivity," *Synthesis* 48 (2016): 3625–3645.

17. D. E. Polat, D. D. Brzezinski, and A. M. Beauchemin, "Formation of Complex Hydrazine Derivatives via Aza-Lossen Rearrangement," *Organic Letters* 21 (2019): 4849–4852.

18. Y. Murakami, Y. Yokoyama, C. Sarakura, and M. Tamagawa, "An Efficient Synthesis of 1, 1-Disubstituted Hydrazines," *Chemical and Pharmaceutical Bulletin* 31 (1983): 423–428.

19. C. D. Bain, J. M. Bayne, D. S. Bohle, I. S. Butler, and J. Poisson, "Synthesis of Reduction-Sensitive 1,1-Diarylhydrazines from 1,1-Diarylamines," *Canadian Journal of Chemistry* 92 (2014): 904–912.

20. D. Pollok and S. R. Waldvogel, "Electro-Organic Synthesis – a 21st Century Technique," *Chemical Science* 11 (2020): 12386–12400.

21. H.-C. Xu and K. D. Moeller, "Electrochemistry in Synthetic Organic Chemistry," *Journal of Organic Chemistry* 86 (2021): 15845–15846.

22. R. D. Little and K. D. Moeller, "Introduction: Electrochemistry: Technology, Synthesis, Energy, and Materials," *Chemical Reviews* 118 (2018): 4483–4484.

23. A. Wiebe, T. Gieshoff, S. Möhle, E. Rodrigo, M. Zirbes, and S. R. Waldvogel, "Electrifying Organic Synthesis," *Angewandte Chemie International Edition* 57 (2018): 5594–5619.

24. S. Möhle, M. Zirbes, E. Rodrigo, T. Gieshoff, A. Wiebe, and S. R. Waldvogel, "Modern Electrochemical Aspects for the Synthesis of Value-Added Organic Products," *Angewandte Chemie International Edition* 57 (2018): 6018–6041.

25. S. B. Beil, D. Pollok, and S. R. Waldvogel, "Reproducibility in Electroorganic Synthesis—myths and Misunderstandings," *Angewandte Chemie International Edition* 60 (2021): 14750–14759.

26. M. C. Leech and K. Lam, "A Practical Guide to Electrosynthesis," *Nature Reviews Chemistry* 6 (2022): 275–286.

27. D. F. Nater, P. Hendriks, and S. R. Waldvogel, "Electrochemical Hofmann Rearrangement at High Current Densities in a Simple Flow Setup," *Molecular Catalysis* 554 (2024): 113823–113829.

28. D. F. Nater, R. Zhao, J. Rocker, et al., "Hectogram-Scale Synthesis of Carbamates Using Electrochemical Hofmann Rearrangement in Flow," *Organic Process Research & Development* 29 (2025): 2370–2377.

29. X. Zhao, J. Wang, D. Guo, et al., "A Novel Electrochemical Hofmann-Type Rearrangement Enables Facile Access to α-Oxoisocyanates for the Synthesis of *N*-Carbamoylacetamides," *Green Chemistry* 27 (2025): 2751–2759.

30. Y. Matsumura, T. Maki, and Y. Satoh, "Electrochemically Induced Hofmann Rearrangement," *Tetrahedron Letters* 38 (1997): 8879–8882.

31. L. Li, M. Xue, X. Yan, W. Liu, K. Xu, and S. Zhang, "Electrochemical Hofmann Rearrangement Mediated by NaBr: Practical Access to Bioactive Carbamates," *Organic & Biomolecular Chemistry* 16 (2018): 4615–4618.

32. M. Wang and P. Wilson, "An Electrochemical Hofmann Rearrangement on Acrylamide Copolymers," *Polymer Chemistry* 14 (2023): 3057–3062.

33. B. K. Malviya, C. Bottecchia, K. Stone, et al., "Multigram Electrochemical Hofmann Rearrangement Using a Spinning Three-Dimensional Anode," *Organic Process Research & Development* 27 (2023): 2183–2191.

34. V. M. Breising, J. M. Kayser, A. Kehl, D. Schollmeyer, J. C. Liermann, and S. R. Waldvogel, "Electrochemical Formation of *N*, N′-Diarylhydrazines by Dehydrogenative N–N Homocoupling Reaction," *Chemical Communications* 56 (2020): 4348–4351.

35. J. C. Bieniek, M. Grünewald, J. Winter, D. Schollmeyer, and S. R. Waldvogel, "Electrochemical Synthesis of *N*, N′-Disubstituted Indazolin-3-Ones via an Intramolecular Anodic Dehydrogenative N–N Coupling Reaction," *Chemical Science* 13 (2022): 8180–8186.

36. E. Feng, Z. Hou, H. Xu, and Chin, Electrochemical-Promoted Synthesis of 2-Thiazolines via Selenylation/Cyclization of N-Allylthioamides," *Journal of Organic Chemistry* 39 (2019): 1424–1428.

37. B. R. Rosen, E. W. Werner, A. G. O. 'Brien, and P. S. Baran, "Total Synthesis of Dixiamycin B by Electrochemical Oxidation," *Journal of the American Chemical Society* 136 (2014): 5571–5574.

38. A. Kehl, T. Gieshoff, D. Schollmeyer, and S. R. Waldvogel, "Electrochemical Conversion of Phthaldianilides to Phthalazin-1,4-Diones by Dehydrogenative N–N Bond Formation," *Chemistry – A European Journal* 24 (2018): 590–593.

39. T. Gieshoff, A. Kehl, D. Schollmeyer, K. D. Moeller, and S. R. Waldvogel, "Insights into the Mechanism of Anodic N–N Bond Formation by Dehydrogenative Coupling," *Journal of the American Chemical Society* 139 (2017): 12317–12324.

40. T. Gieshoff, D. Schollmeyer, and S. R. Waldvogel, "Access to Pyrazolidin-3,5-Diones through Anodic N–N Bond Formation," *Angewandte Chemie International Edition* 55 (2016): 9437–9440.

41. S. R. Waldvogel and B. Janza, "Renaissance of Electrosynthetic Methods for the Construction of Complex Molecules," *Angewandte Chemie International Edition* 53 (2014): 7122–7123.

42. L. G. Gombos, J. Nikl, and S. R. Waldvogel, "Dual Roles of Supporting Electrolytes in Organic Electrosynthesis," *ChemElectroChem* 11 (2024): e202300730.

43. O. A. Levitskiy, D. A. Dulov, O. M. Nikitin, et al., "Competitive Routes for Electrochemical Oxidation of Substituted Diarylamines: The Guidelines," *ChemElectroChem* 5 (2018): 3391–3410.

44. M. Dörr, M. M. Hielscher, J. Proppe, and S. R. Waldvogel, "Electrosynthetic Screening and Modern Optimization Strategies for Electrosynthesis of Highly Value-Added Products," *ChemElectroChem* 8 (2021): 2621–2629.

45. D. R. Lide, "CRC Handbook of Chemistry and Physics", can be found under https://ia601308.us.archive.org/27/items/CRC.Press.Handbook.of.Chemistry.and.Physics.85th.ed.eBook-LRN/CRC.Press.Handbook.of.Chemistry.and.Physics.85th.ed.eBook-LRN.pdf, (2005), (accessed: February, 2026)

46. H. Paulsen and Stoye D., *Amides*, J. Zabicky (Wiley, 1970), 515–600.

47. H. Pletsch, Y. Lyu, and D. P. Halter, "Ex Situ Electro-Organic Synthesis – a Method for Unrestricted Reaction Control and New Options for Paired Electrolysis," *ChemElectroChem* 11 (2024): e202400489.

48. F. Sprang, N. Schupp, P. J. Kohlpaintner, L. J. Gooßen, and S. R. Waldvogel, "E-Dakin Reaction: Oxidation of Hydroxybenzaldehydes to Phenols with Electrochemically Generated Peroxodicarbonate as Sustainable Ex-Cell Oxidizer," *Green Chemistry* 26 (2024): 5862–5868.

49. R. D. Taylor, M. MacCoss, and A. D. G. Lawson, "Rings in Drugs," *Journal of Medicinal Chemistry* 57 (2014): 5845–5859.

50. E. Vitaku, D. T. Smith, and J. T. Njardarson, "Analysis of the Structural Diversity, Substitution Patterns, and Frequency of Nitrogen Heterocycles among U.S. FDA Approved Pharmaceuticals," *Journal of Medicinal Chemistry* 57 (2014): 10257–10274.

51. Y. He, Z. Zheng, J. Yang, X. Zhang, and X. Fan, "Recent Advances in the Functionalization of Saturated Cyclic Amines," *Organic Chemistry Frontiers* 8 (2021): 4582–4606.

52. A. M. Soliman, H. M. Karam, M. H. Mekkawy, and M. M. Ghorab, "Antioxidant Activity of Novel Quinazolinones Bearing Sulfonamide: Potential Radiomodulatory Effects on Liver Tissues via NF-κB/ PON1 Pathway," *European Journal of Medicinal Chemistry* 197 (2020): 112333–112346.

53. H. Fan and Y. Xie, Wigen Biomedicine Technology Shanghai Co Ltd, WO 2020173417A1, (2020).

54. B. Cao, L. Zhao, G. Dou, et al. Shenzhen Zhongge Biological Technology Co Ltd, WO 2024032501A1, (2024).

55. W. Zhong, K. Wang, Z. Hu, et al. Qilu Regor Therapeutics Inc, WO 2022140427A1, (2022).

56. Deposition numbers 2493411 (for int) and 2493412 (for 2a) contain the supplementary crystallographic data for this paper. These data are provided free of charge by the joint Cambridge Crystallographic Data Centre and Fachinformationszentrum Karlsruhe Access Structures service.

57. The stoichiometry of the base (4.4 equiv.) was calculated according to the standard reaction conditions, in which a total charge of 4.4 F mol^{-1} was applied. Thus, 4.4 equiv. of methoxide is theoretically generated at the cathode during electrolysis.

58. G. Sun, H. Sun, Y. Zhang, and L. Zhang, Wuxi Sanger Biotechnology Co Ltd, CN 113683584A, (2021).

59. V. R. Regalla, R. R. Addada, and A. Chatterjee, "Copper(II)-Catalyzed-α-C(sp^3)-H Activation of Cyclic Amines: A Simple and Efficient Strategy for the Synthesis of Fused Pyrazole Derivatives," *Tetrahedron Letters* 59 (2018): 4161–4164.

60. J. Seidler, J. Srtugatchi, T. Gärtner, and S. R. Waldvogel, "Does Electrifying Organic Synthesis Pay off? the Energy Efficiency of Electro-Organic Conversions," *MRS Energy & Sustain* 7 (2020): E42.

61. W. Gagné-Monfette, J.-F. Vincent-Rocan, O. C. Lutes, et al., "Investigation of Masked *N*-Acyl-N-Isocyanates: Support for Oxadiazolones as Blocked n-Isocyanate Precursors," *Chemistry – A European Journal* 27 (2021): 14051–14056.

62. C. Gütz, A. Stenglein, and S. R. Waldvogel, "Highly Modular Flow Cell for Electroorganic Synthesis," *Organic Process Research & Development* 21 (2017): 771–778.

63. A. H. Christian, S. Jia, W. Cao, et al., "A Physical Organic Approach to Tuning Reagents for Selective and Stable Methionine Bioconjugation," *Journal of the American Chemical Society* 141 (2019): 12657–12662.

64. L. Tiwari, V. Kumar, B. Kumar, and D. Mahajan, "A Practically Simple, Catalyst Free and Scalable Synthesis of *N*-Substituted Ureas in Water," *Rsc Advances* 8 (2018): 21585–21595.

65. C. E. Spivak, J. S. Yadav, W. C. Shang, M. Hermsmeier, and T. M. Gund, "A Practically Simple, Catalyst Free and Scalable Synthesis of *N*-Substituted Ureas in Water," *Journal of Medicinal Chemistry* 32 (1989): 305–309.

66. J. Vaith, D. Rodina, G. C. Spaulding, and S. M. Paradine, "Pd-Catalyzed Heteroannulation Using *N*-Arylureas as a Sterically Undemanding Ligand Platform," *Journal of the American Chemical Society* 141 (2022): 6667–6673.

67. P. Di Fruscia, K.-K. Ho, S. Laohasinnarong, et al., "The Discovery of Novel 10,11-Dihydro-5*H*-Dibenz[b,f]azepine SIRT2 Inhibitors," *MedChemComm* 3 (2012): 373–378.

68. D. Most and K. Rossen, Evonik Operations GmbH Sanofi Aventis France, WO 2006094920A2, (2006).

69. M. Ilisson, K. Tomson, A. Selyutina, S. Türk, and U. Mäeorg, "Synthesis of Novel Saccharide Hydrazones," *Synthetic Communications* 45 (2015): 1367–1373.

Supporting Information

Additional supporting information can be found online in the Supporting Information section. **Supporting Fig. S1:** Flow cell disassembled (top) and reaction setup (bottom). **Supporting Fig. S2:** Pareto chart for analyzing the individual and synergistic effects of different factors. **Supporting Fig. S3:** Main effect plots. **Supporting Fig. S4:** ORTEP-plot of the two crystallographically independent molecules of int drawn at the 40% probability level. **Supporting Table S1:** Investigated factors and ranges. **Supporting Table S2:** Performed screening experiments. **Supporting Table S3:** Optimization of c and Q. **Supporting Table S4:** Optimization of current density. **Supporting Table S5:** Optimization of solvent mixture. **Supporting Table S6:** Optimization of concentration of substrate. **Supporting Table S7:** Optimization of addition of MeONa. **Supporting Table S8:** Optimization of supporting electrolytes. **Supporting Table S9:** Optimization of concentration of lithium chloride. **Supporting Table S10:** Crystallographic data for 2a. **Supporting Table S11:** Crystallographic data for int. The authors have cited additional references within the Supporting Information [18, 62–69].